



Equilibrium and kinetics studies for the adsorption of Basic Red 46 on nickel oxide nanoparticles-modified diatomite in aqueous solutions



Reza Khalighi Sheshdeh^{a,*}, Mohammad Reza Khosravi Nikou^a, Khashayar Badii^b, Nargess Yousefi Limaee^b, Gelayol Golkarnarenji^c

^a Gas Engineering Department, Ahwaz Faculty of Petroleum, Petroleum University of Technology (PUT), P.O. Box: 63431, Ahwaz, Iran

^b Department of Environmental Researches, Institute for Color Science and Technology (ICST), P.O. Box: 16765-654, Tehran, Iran

^c Institute for Frontier Materials, Deakin University, Geelong VIC 3220, Australia

ARTICLE INFO

Article history:

Received 7 October 2013

Received in revised form 27 January 2014

Accepted 25 February 2014

Available online 26 March 2014

Keywords:

Adsorption

Diatomite

Nickel oxide nanoparticles

Isotherm

Kinetics

Basic Red 46

ABSTRACT

The nickel oxide nanoparticles-modified diatomite (NONMD) as a low-cost adsorbent was investigated for the removal of C.I. Basic Red 46 (BR46) from aqueous solution. Various physico-chemical parameters were studied such as solution pH, adsorbent dosage, adsorbent size, initial dye concentration, temperature, contact time and salt (NaCl, NaHCO₃ and Na₂SO₄). The mean size and the surface morphology of the adsorbent were characterized by SEM, BET, FTIR, XRD, EDX and elemental analysis. The maximum percentage of BR46 dye removal from aqueous solution was 99.48% (124.35 mg/g) when 0.005 g of NONMD was applied at pH 8, temperature 25 ± 1 °C, agitation speed of 200 rpm, initial dye concentration of 25 mg/L, and a mixing time of 60 min. Furthermore, under the same conditions, the maximum adsorption of dye on raw diatomite was 84.49% (105.61 mg/g). The experimental data showed that the adsorption of dye on raw diatomite follows the Langmuir model, but its adsorption on modified diatomite followed the BET model. The kinetics results were found to conform well to pseudo-second order kinetics model with good correlation. Thus, this study demonstrated that the NONMD could be used as a low-cost natural adsorbent for removal of BR46 from aqueous solution.

© 2014 Taiwan Institute of Chemical Engineers. Published by Elsevier B.V. All rights reserved.

1. Introduction

Synthetic dyes have increasingly been used in the textile and dyeing industries because of their ease and cost-effectiveness in synthesis as well as high stability to light, temperature, detergent and microbial attack which can lead to the discharge of highly polluted effluents [1]. More than 10,000 chemically different dyes are being manufactured, and the world dyestuff and dye intermediates production are estimated to be around 7×10^8 kg per annum [2,3]. Colour as one of the effluent characteristics affects the nature of the water, inhibits sunlight penetration into the stream and reduces the photosynthetic activity [4,5]. Moreover, some dyes are carcinogenic and mutagenic which are generally stable to biological degradation [4,6]. Hence, their removal from aqueous solution, before discharging them into the environment is extremely important [7]. Therefore, the development of efficient,

low-cost and environmentally friendly technologies to reduce dye content in wastewater is extremely necessary.

New economical, locally available and highly effective biosorbents are still under development. Furthermore, many treatment systems have been proposed for the removal of synthetic dyes from aqueous solutions. Coagulation [8], flocculation [9], photocatalytic degradation [10–12], membrane filtration [13], microbiological decomposition [14], electrochemical oxidation [15], fungus biosorbent [16] and adsorption [17–25] are the most commonly used methods for removing dyes from waste and effluent systems. The microbiological, photocatalytic and electrochemical decomposition procedures are not efficient because many dyes cannot be easily decomposed [15]. Adsorption is considered to be particularly competitive, economically efficient and cost-effective process for the removal of dyes, heavy metals and other organic and inorganic hazardous impurities from aqueous solutions. Although activated carbon is the most efficient and popular adsorbent and has been used with great success, the high cost of activated carbon sometimes restricts its application with regard to dye removal [26–33]. Recently, many researchers have attempted to use alternative low-cost sorbents to replace

* Corresponding author. Tel.: +98 611 5550868; fax: +98 611 5550868.

E-mail address: rezakhalighi@yahoo.com (R. Khalighi Sheshdeh).

Symbols used

C_0	[mg/L] initial concentration of BR46
C_e	[mg/L] residual concentration at equilibrium
C_s	[mg/L] saturation concentration of BR46
$K_{1,ad}$	[1/min] rate constant of Pseudo-first-order
$K_{2,ad}$	[1/min] rate constant of Pseudo-second-order
k_F	[–] Freundlich constant
k_L	[–] Langmuir constant
k_b	[–] BET constant
m	[g] mass of adsorbent used
n	[–] parameter indicating the intensity of adsorption
q_e	[mg/g] residual amount adsorbed at equilibrium
$q_{e,exp}$	[mg/g] experimental residual amount adsorbed at equilibrium
q_p	[mg/g] predicted sorption capacity
q_o	[mg/g] observed sorption capacity
Q_0	[mg/g] maximum sorption capacity
r^2	or R^2 [–] correlative coefficient for all models
T	[K] absolute temperature
t	[min] contact time
V	[L] volume of BR46 solution

with activated carbons. Some of these alternative biosorbents are banana pith [34], vine [35], eucalyptus bark [36], neem leaf powder [37], *Luffa cylindrica* fiber [38], sunflower seed hull [39], soy meal hull [40], hazelnut shell [41] and neem sawdust [17]. Nevertheless, the adsorption capacities of most of the above adsorbents were still limited.

BR46 was selected as a model synthetic azo dye due to its extensive use in the textile industry. Azo dyes are a class of dyes characterized by the presence of the azo group. Due to high usage of these dyes, large volumes of coloured effluents are discharged into the environmental and water resources. The release of azo dyes into the environment is of concern due to their toxicity, mutagenicity and carcinogenicity [42]. Hence, removal of azo dyes from wastewater is a major environmental issue.

Diatomite ($\text{SiO}_2 \cdot n\text{H}_2\text{O}$) is made up principally from the skeletons of aquatic plants called diatom that usually is a pale-coloured, soft, lightweight siliceous sedimentary rock [43]. Diatomite contains a wide variety of shape and sized diatoms, typically 10–200 μm , in a structure including up to 80–90% pore spaces [42,43]. Diatomite's extremely porous structure, low density and high surface area make it suitable as an adsorbent for the removal of organic and inorganic chemicals. Diatomite is found in abundance in Iran. Several studies have been carried out on the use of diatomite as an adsorbent for removing some contaminants such as heavy metals [44], basic dye (Methylene blue) [17], basic and reactive dyes (Methylene blue, reactive black, reactive yellow) [45] and some textile dyes (Sif Blau BRF, Everzol Brill Red 3BS, Int Yellow 5GF) [45]. Furthermore, the unique properties of diatomite caused its applications as filtration media in a number of industries [46]. Diatomite is approximately 500 times cheaper than commercial activated carbon [46] and has the potential of being successfully used as a cost-effective alternative to activated carbon.

In the present investigation, the utilization possibility of nickel oxide nanoparticles-modified diatomite (NONMD) as an adsorbent for the removal of BR46 dye from an aqueous medium has been studied. Nickel metal can be a good choice for degrading the dyes and other pollutants from aqueous solutions [47]. Table 1 shows

Table 1

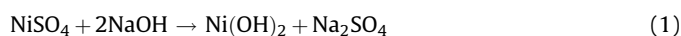
The comparison between different kinds of adsorbent for the adsorption of BR46.

Adsorbent	Maximum adsorption capacity (mg/g)	References
Raw Diatomite	83.67	In this work
NONMD	98.16	In this work
Pine tree leaves	71.94	[48]
Princess tree leaf	43.10	[49]
Moroccan clay	54	[50]
Boron industry waste	74.73	[51]
Gypsum	39.17	[52]

the comparison between maximum monolayer sorption capacities (mg/g) of different adsorbents for the adsorption of BR46. As it is evident, the maximum adsorption capacity of used adsorbents (in this study) is more than others. The equilibrium and kinetics study are investigated and the effects of various process parameters such as pH, contact time, initial dye concentration, calcinations and sorbent dosage on the adsorption process were examined. Equilibrium data are attempted by various adsorption isotherms including Langmuir, Freundlich and Brunauer–Emmett–Teller (BET) isotherms in order to select an appropriate isotherm model. Moreover, a kinetics study of the adsorption process is also considered to describe the rate of sorption.

2. Experimental procedure**2.1. Preparation of adsorbent**

Diatomite sample was obtained from Tabriz, Iran. The sample was washed several times with distilled water and HCl (1 M) to remove fines and other adhered impurities and to achieve neutralization. Moreover, in the acidic conditions nickel nanoparticles can put better on the surface of diatomite. The sample was finally filtered, dried at 60 °C for 24 h, and stored in closed containers for further use. The nanoparticles of NiO were synthesized by using following reaction:



The nanoparticles of NiO were synthesized by adding NiSO_4 and NaOH (1 M) to the solution. It means that 2.0 g of previously dried diatomite (raw diatomite) were added to 25 ml of Nickel hydroxide (1 M) and the sample was stirred in the agitation speed of 200 rpm for 1 h. The new material (mixture of Ni and diatomite) was sequentially separated by filtration that the product of this reaction was Ni(OH)_2 . The final product that was mixture of raw diatomite and Ni(OH)_2 had to be put in the furnace, by that Ni(OH)_2 changed to NiO and mixed by raw diatomite. The calcination process was carried out by placing NONMD sample in the furnace at 250 °C for 4.5 h. The sample was then allowed to cool in a desiccator. The modified sample was used to examine the effect of silanol groups and the role of pore size distribution on the adsorption process. It is clear from the FT-IR spectra and EDX analysis, the raise of metal oxide content at the modified diatomite can be the main reason for increasing the adsorption capacity. In industries, there are many heavy metals contaminated materials. Recovery of materials and clean up these contaminations is very difficult and expensive [48–52]. Our investigation is a key to change a poisonous industrial waste to a valuable by product.

2.2. Reagents and solutions

BR46 dye was obtained from Ciba Ltd. and was used without further purification. The chemical structure of this dye is shown in

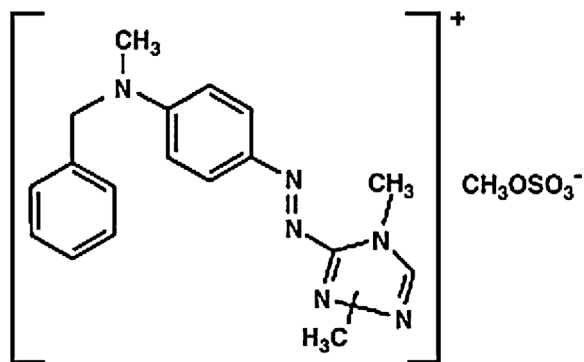


Fig. 1. The chemical structure of BR46 dye.

Fig. 1. Distilled water was throughout employed as solvent. The pH measurements were made using Hach pH meter. The pH adjustments of the solution were made by adding a small amount of HCl or NaOH (1 M). These chemicals were of analar grade and purchased from Merck, Germany.

2.3. Adsorption procedure

The adsorption experiments were performed by mixing various amounts of diatomite (0.001–0.05 g) in 25 mL of dye solutions with varying concentrations (ranging from 25 to 55 mg/L) at various pH (2–12). The pH studies were carried out to determine the optimum pH at which maximum dye removal could be achieved with diatomite. Adsorption experiments were conducted at various concentrations of dye solutions (25, 35, 45 and 55 mg/L) using optimum amount of diatomite (0.005 g) at pH 8, an agitation speed of 200 rpm and temperature 25 ± 1 °C for 1 h to attain equilibrium conditions. The changes of absorbance were determined at certain time intervals (5, 10, 30, 60, 90 and 120 min) during the adsorption process. After adsorption experiments, the dye solutions were centrifuged for 10 min in a Hettich EBA20 centrifuge at 4000 rpm in order to separate the sorbent from the solution and dye concentration was then determined.

The amount of dye adsorbed at equilibrium, q_e (mg/g), was calculated using the following equation:

$$q_e = \frac{(C_0 - C_e)V}{M} \quad (2)$$

where C_0 and C_e (mg/L) are the initial and equilibrium concentrations of dye, respectively, V (L) is the volume of the dye solution and M (g) is the adsorbent mass.

2.4. Analysis

The residual dye concentrations in aqueous medium were determined using a Perkin–Elmer spectrophotometer corresponding to maximum wavelength (λ_{max}) of BR46 dye. The XRD analysis was performed on raw and modified diatomite samples using a Philips Xpert x-ray diffractometer. Scanning electron microscopy (SEM) of both raw and modified diatomite were carried out using LEO 1455VP scanning electron microscope before and after modification process. The samples were coated with gold (Au) prior to the scanning in the electron microscope. By using nitrogen adsorption method, the BET specific surface area of adsorbents was measured, using Autosorb-1MP apparatus from Qantachrome at 77 K. The analysis on compositions was determined by energy dispersive X-ray technique using EDX-System (Tescan Vega/2/Instrument) which is fitted to the SEM instrument.

3. Results and discussion

3.1. Surface characterization

As the calcination process decreases the diatomite capacity for the removal of dye from aqueous solutions, therefore in this investigation, we decided to compare adsorption properties of modified diatomite with raw diatomite instead of calcined diatomite. In order to explore the surface characteristics of diatomite, a Fourier Transformed Infra-Red (FTIR) analysis was performed in the range of 450–4000/cm. Fig. 2 shows the FTIR spectra of raw and modified diatomite samples before the adsorption process and Fig. 3 shows the FTIR spectra of raw and modified diatomite samples after the adsorption process. In the first spectrum (curve 'a' in Fig. 2), the peaks at major adsorption bands were observed at 3622, 3421, 2506, 1636, 1038, 915, 794, 692, 671, 627, 596, 522 and 470/cm. The peaks at 3622 and 3421/cm illustrate the (H) atom that is attached to heteroatoms (Si–H), the peaks at 2506 cm^{-1} is due to the free silanol group (Si–O–H), the peak at 1636/cm represents (H–O–H) bending vibration of water, and the peak at 1038/cm reflects the siloxane (–Si–O–Si–) group stretching. The peaks at 915 and 794/cm correspond to (Si–O–H) vibration. The peaks of 692, 671, 627, 596, 522 and 470/cm are attributed to the Si–O–Si bending vibration. The peaks of the major bands in the spectrum of NONMD (mentioned as 'b' in Fig. 2) and raw diatomite are similar, except in fingerprint region (from 1500 to 500/cm). Although the nickel content of NONMD is too low, there is a recognisable difference in this region regarding to nickel oxide nanoparticles on diatomite [53]. In addition, Figs. 2a and b illustrate that the amount of silanol group has decreased slightly, and the metal oxide content has risen at the modified diatomite; however, the adsorption capacity has increased at NONMD.

Comparison of Figs. 2 and 3 shows slight reduction on peaks' transmittance of silanol, siloxane, and metal oxide groups in raw diatomite and NONMD. Besides, appearance of peak at 1871/cm

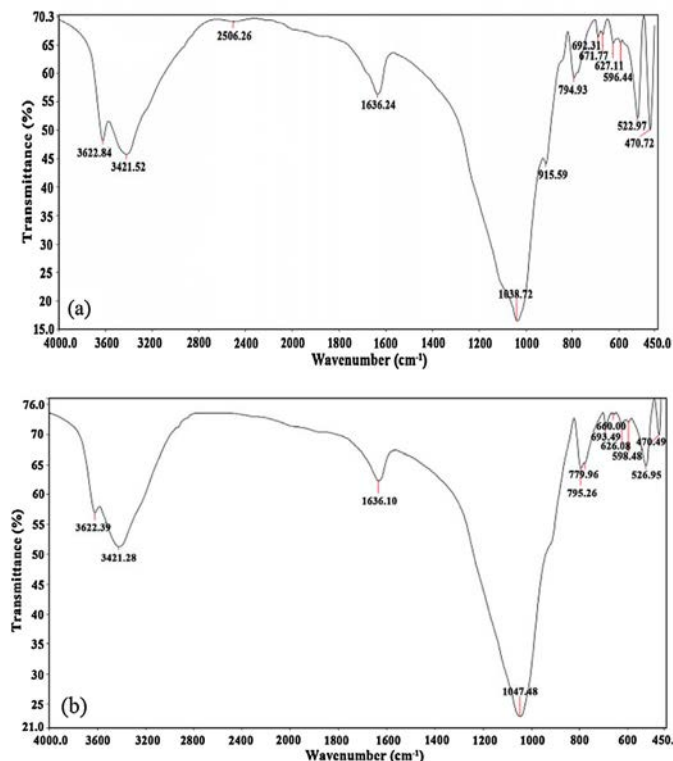


Fig. 2. FT-IR spectra of adsorbents before adsorption (a) raw and (b) NONMD.

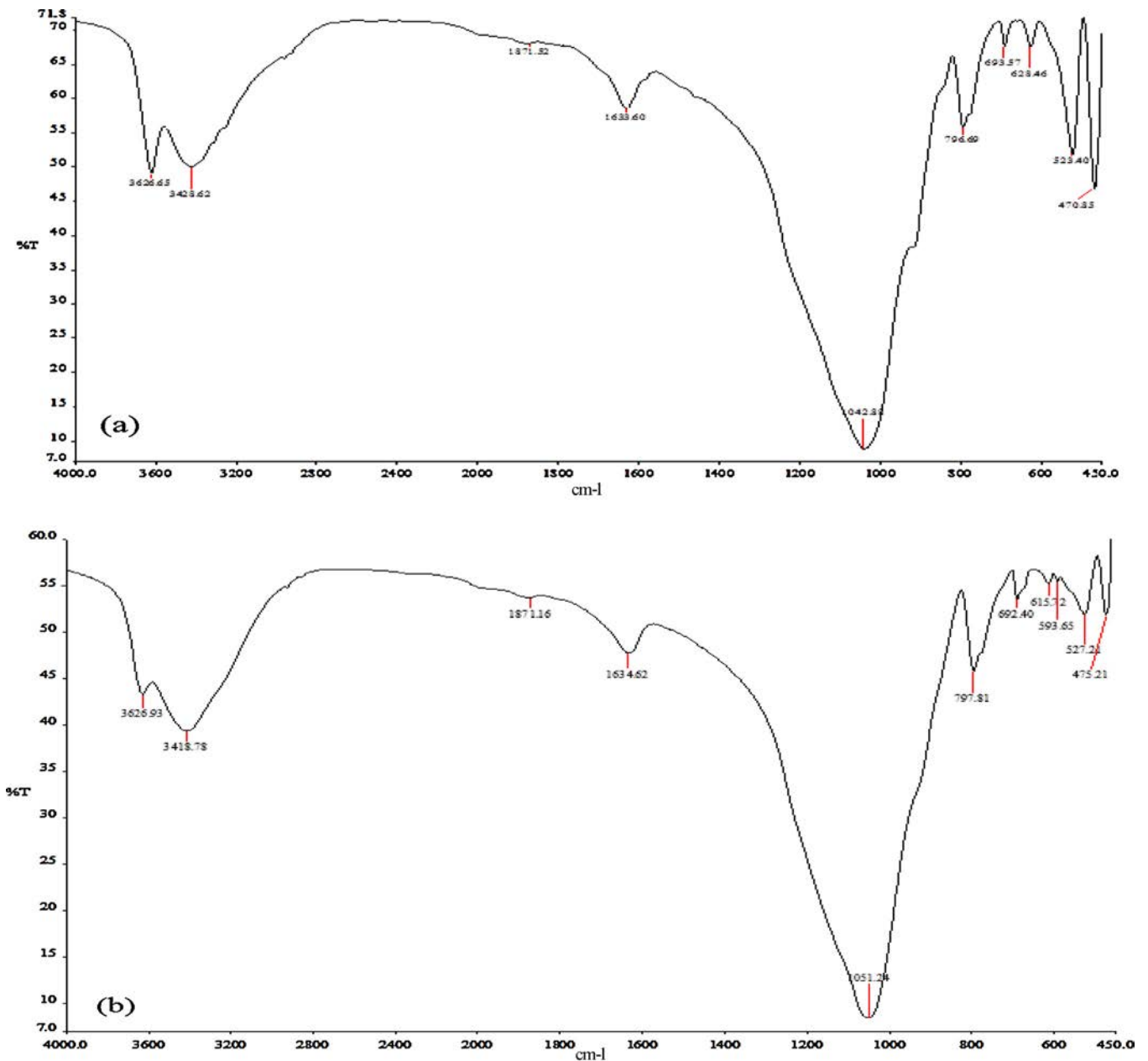


Fig. 3. FT-IR spectra of adsorbents after adsorption (a) raw and (b) NONMD.

(Fig. 3) illustrates the adsorption of dye (combi group of aromatic rings) on both adsorbents.

Scanning electron micrographs (SEM) of raw and modified diatomite, before and after the adsorption process, are shown in Fig. 4. These figures present that raw diatomite particles are amorphous, their pore spaces are lower than modified adsorbent, and particles of NONMD are more uniform and geometrical significantly. After modification and calcination process at 250 °C, the structure of the adsorbent changed from amorphous sheets to semi-sphere shapes. Therefore, the volume of the pore spaces has increased, and the surface functional groups of modified diatomite have improved. Hence, the diffusion resistance of adsorption process has decreased, and the kinetics and capacity of dye adsorption process have risen. Moreover, adsorption of dye has caused a sticky phenomenon on structure of both adsorbents.

XRD and EDX analysis results of the raw and modified diatomite are shown in Figs. 5 and 6 respectively. It can be seen from both of

them that the x-ray pattern of the raw diatomite is different from the pattern of the modified diatomite, suggesting that a phase transformation probably occurred during the calcinations process. The main composition of raw diatomite is quartz, anorthite and muscovite. It is evident that sanidine was appeared; while anorthite and muscovite were completely removed as the diatomite was calcined at 250 °C.

The composition analysis was determined by energy dispersive x-ray technique using EDX-System (Fig. 6). As is evident from Fig. 6, the raw diatomite did not have any Nickel but after modification process Ni was appeared (3.96%W). In fact, some peaks in the diatomite disappeared and some peaks were created by modification process by nickel nanoparticles. Similar behaviour was previously investigated by other researchers [20].

The surface area of the diatomite was determined by BET method. By using nitrogen adsorption method, the BET specific surface area of adsorbents was measured, using Autosorb-1MP

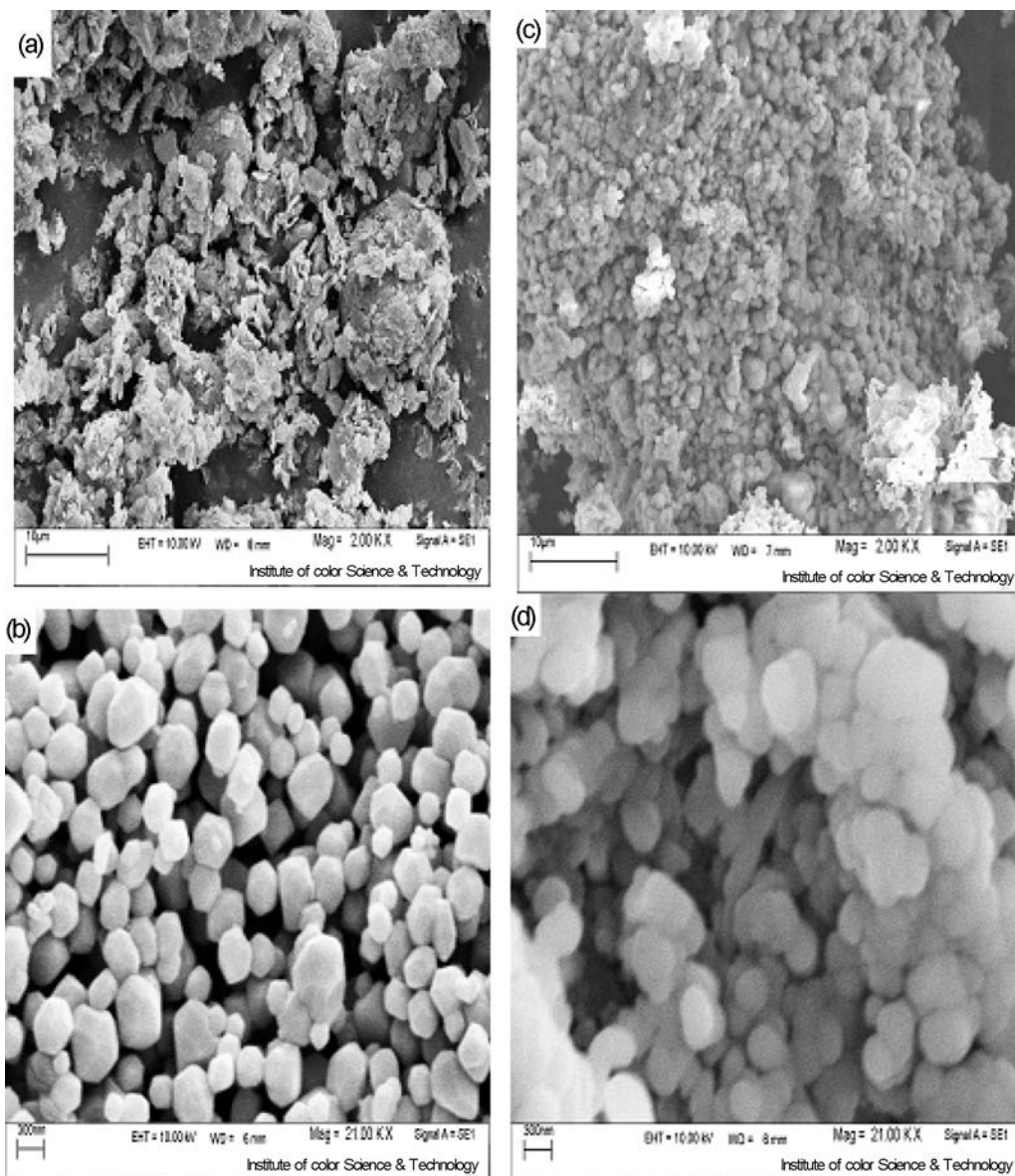


Fig. 4. Scanning electron micrographs before adsorption (a) raw and (b) NONMD, after adsorption (c) raw and (d) NONMD.

apparatus from Qantachrome at 77 K. In this investigation, the values of 7.5 and 28.45 m^2/g were calculated for raw and modified diatomite respectively.

3.2. Effect of adsorbent dosage

The effect of raw and modified diatomite dosage on the adsorption of BR46 dye was investigated at $25 \pm 1^\circ\text{C}$ by varying the adsorbent amount from 0.001 to 0.05 g while keeping the volume of dye solution constant equal to 25 mL, with an initial dye concentration of 25 mg/L. Fig. 7 shows the removal of BR46 dye (mmol/g) versus adsorbent dosage (g/L). The effect of adsorbent dose ranging from 0.04 to 2 g/L on basic red 46 adsorption is given in Fig. 7. As seen from Fig. 7, adsorption capacity for BR 46 decreased with dosage increasing. This may be due to the decrease in the total sorption surface area available to BR 46 resulting from overlapping or aggregation of sorption sites [54]. Similar behaviour for the effect of adsorbent dosage on the dye adsorption capacity was observed and discussed for different types of adsorbents by other researchers [55,56]. Based on the results shown in Fig. 7, 0.005 g of the raw diatomite and NONMD was used for further experiments.

3.3. Effect of initial dye concentration

The effect of initial dye concentration in the range of 5–55 mg/L on adsorption of the BR 46 was investigated and is shown in Fig. 8. The adsorption capacity increased from 0.072 to 0.594 and 0.077 to 0.754 mmol/g for raw diatomite and modified diatomite respectively with increasing of the initial dye concentration. This is probably due to the increase in the driving force of the concentration gradient, as an increase in the initial dye concentration. Similar results were reported by other researchers for banana pith [34] and vine [35].

3.4. Effect of contact time

The adsorption of BR46 dye onto diatomite was evaluated as a function of contact time. Fig. 9 shows the effect of contact time on the percentage removal of BR46 dye in the aqueous phase by raw (Fig. 9a) and NONMD (Fig. 9b). The initial dye concentration was varied from 25 to 55 mg/L. At all initial dye concentrations investigated, the adsorption occurs very fast initially. After 5 min of adsorption process, dye removal by raw diatomite reaches

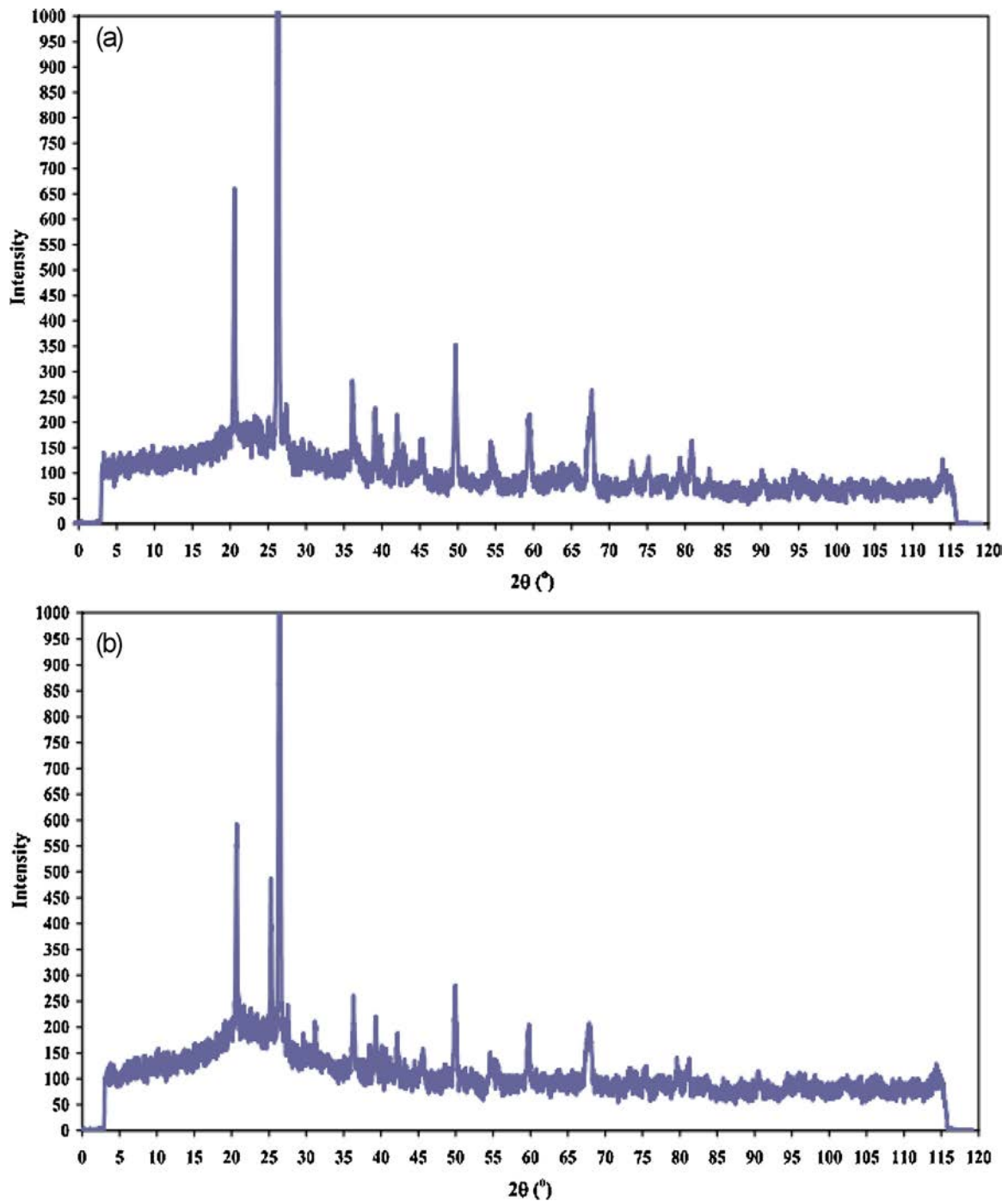


Fig. 5. XRD patterns of (a) raw and (b) NONMD.

51.58 and 56.74% for initial dye concentrations of 25 and 35 mg/L respectively.

As illustrated in Fig. 9b, the adsorption is also fast at early stage of the adsorption process for NONMD. Typically about 80.20% of the ultimate adsorption of BR46 dye with an initial concentration of 25 mg/L takes place within the first 5 min of contact and it almost remains constant thereafter. It means that the most of mass transfer resistance is in bulk of fluid and high rate agitation would decrease this resistant [57]. In addition, these results show that the most of the dye molecules are adsorbed on the external surface of the adsorbent, and transferred to the pores and internal surfaces layer. More experiments are necessary to be carried out to prove this investigation.

3.5. Effect of pH

The pH is the most important factor affecting the adsorption process. The pH studies were conducted to determine the optimum pH at which maximum colour removal could be achieved with diatomite for BR46 dye. The effect of pH was observed by studying the adsorption of dye over a broad pH range of 2–12. The results are shown in Fig. 10. In the present work, as depicted in Fig. 10, for both raw and modified diatomite the highest sorption (99.48% for modified diatomite and 84.49% for raw diatomite) were achieved at pH 8. Therefore, pH 8 was selected as optimum pH for further experiments. At pH < 6 the dye removal of basic red 46 was low that the lower adsorption yield could be due to the fact that the

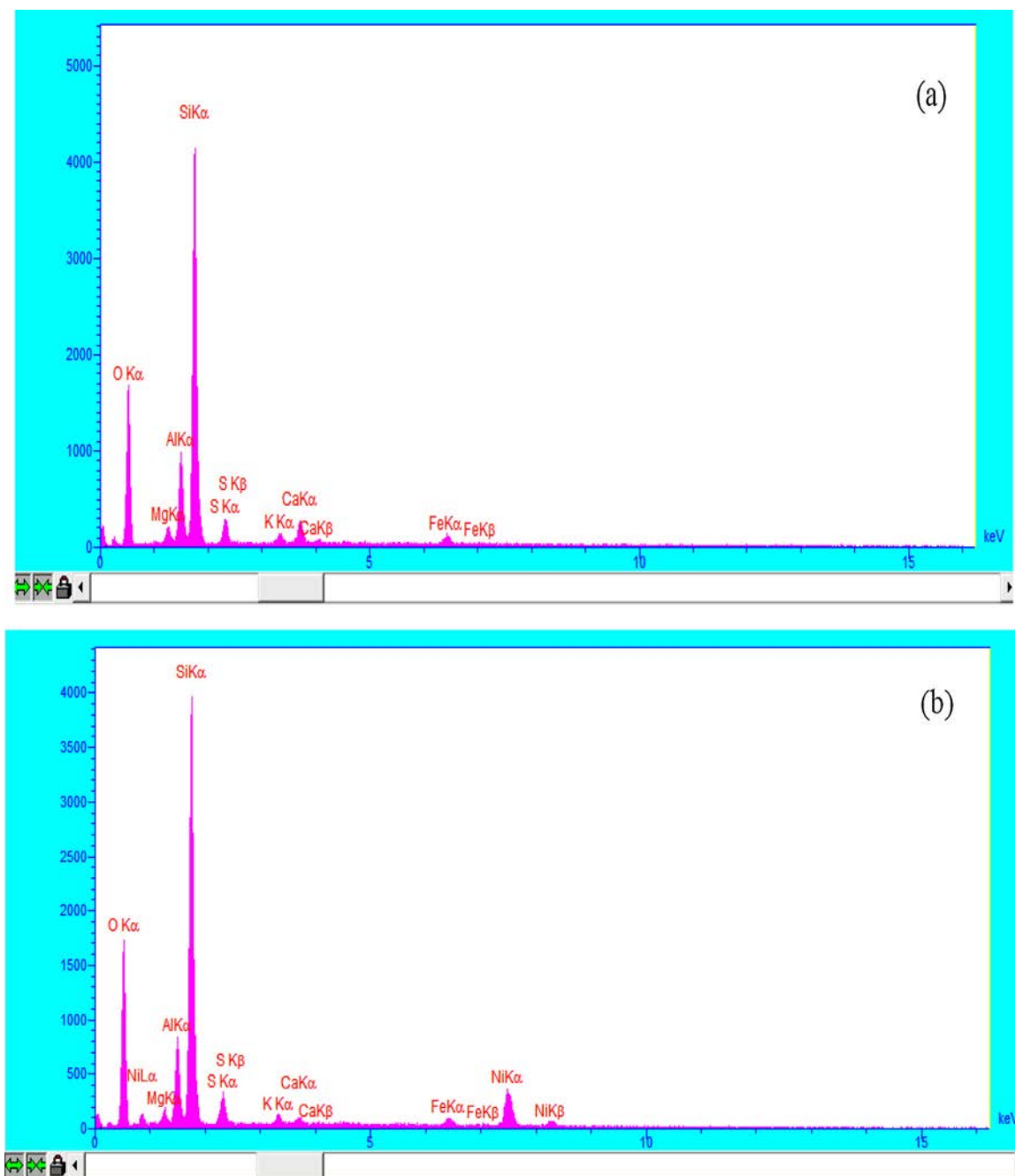


Fig. 6. EDX patterns of (a) raw and (b) NONMD.

hydronium ions with positive charge was abundantly available and thus the competition occurs for the binding to the surface of the sorbent between the hydronium ions and cationic species in the aqueous solution. From pH 6 to 8, the dye removal increased and reached to 99.48% for NONMD and 84.49% for raw diatomite at pH 8.

The adsorption of BR46 dye decreased from 99.48 to 74% with increasing pH of dye solution from 8 to 12 when NONMD was used as an adsorption medium, whereas, the quantity of dye adsorbed decreased from 84.49 to 53.83% in the pH range of 8–12 using raw diatomite as an adsorbent, decrease in adsorption at higher pH ($\text{pH} > 8$) could be attributed to the competition for the sorption sites between hydroxyl ions and predominant the anionic species in aqueous solution. Similar behaviour was previously investigated by other researchers [19,31,35].

3.6. Effect of temperature

The temperature has a significant effect on the adsorption process. Increasing the temperature will change the equilibrium capacity of the adsorbent for a particular adsorbate. Furthermore, an increase in temperature can raise the rate of dye molecules diffusion in the internal pores of the adsorbent [22]. In this study, the removal of BR46 dye from aqueous solution using diatomite has been investigated at four different temperatures ranged from 25 to 55 °C.

By increasing temperature, the adsorption efficiency of the NONMD has extended from 0.384 to .407 (mmol/g). Therefore, the remediation process incorporating adsorption method can be performed under normal temperature for an industrial scale. It was well depicted in Fig. 11 that the adsorption process was not

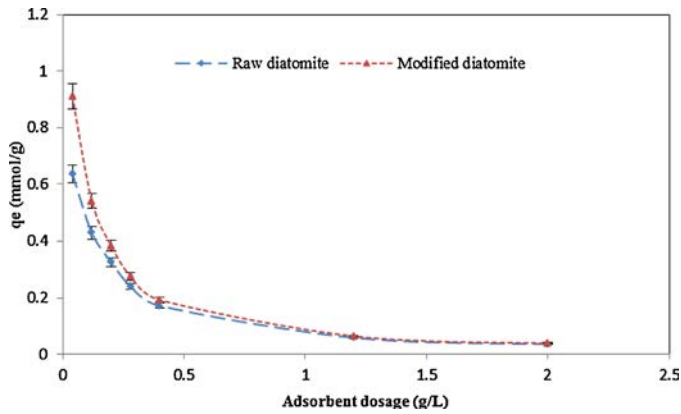


Fig. 7. Effect of adsorbent dosage, temperature = 25 ± 1 °C, initial dye concentration = 25 mg/L, pH = 8, contact time = 60 min, agitation speed = 200 rpm.

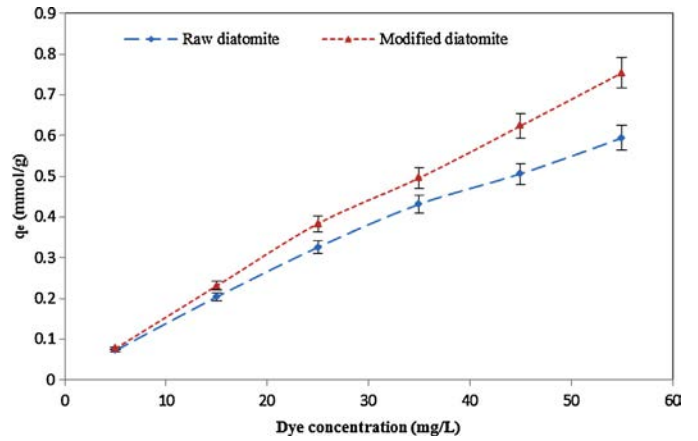


Fig. 8. Effect of initial dye concentration, contact time = 60 min, temperature = 25 ± 1 °C, pH = 8, agitation speed = 200 rpm.

sensitive to the temperature. It was shown that the energy balance was not important in this process [56–58].

3.7. Effect of salt concentration

The occurrence of salts is common in coloured wastewater [58]. Inorganic anions of salts may compete for the active sites on the adsorbent surface or deactivate the adsorbent. Thus dye adsorption efficiency decreases. An important limitation resulting from the high reactivity and non-selectivity of adsorbent is that it also reacts with non-target compounds present in the wastewater such as dye

auxiliaries present in the exhausted dye bath. It results in higher adsorbent dosage demand to accomplish the desired degree of dye removal efficiency.

To investigate the inorganic salts effect on dye removal efficiency, 0.001 mole of Na_2SO_4 , NaHCO_3 and NaCl were added to the dye solution. Fig. 12 illustrates that the dye removal capacity by NONMD is decreased in the presence of salts because these salts have small molecules and compete with dyes in adsorption onto NONMD. Similar behaviour was previously investigated by other researchers [13,57,58].

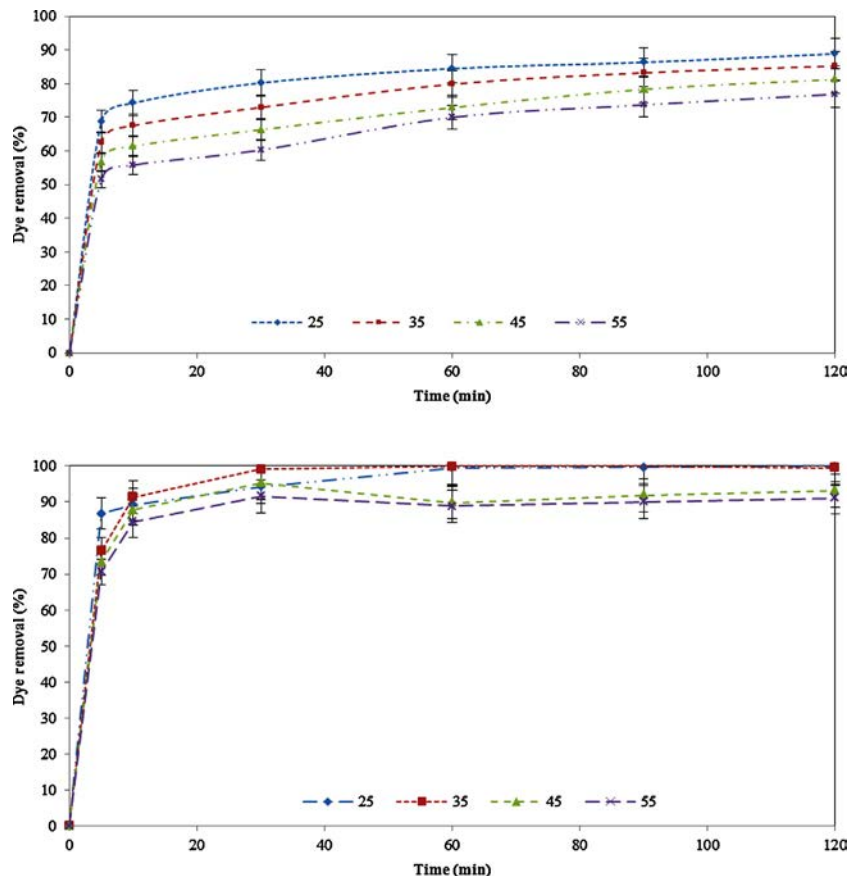


Fig. 9. Effect of contact time (a) raw and (b) NONMD, pH = 8, agitation speed = 200 rpm, adsorbent dosage = 0.005 g.

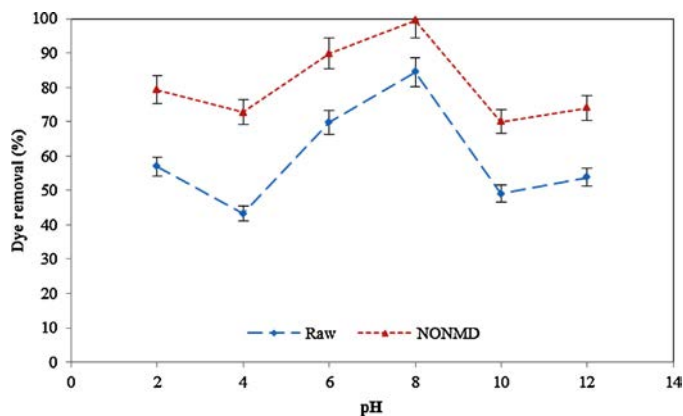


Fig. 10. Effect of pH, agitation speed = 200 rpm, temperature = 25 ± 1 °C, equilibrium time = 60 min.

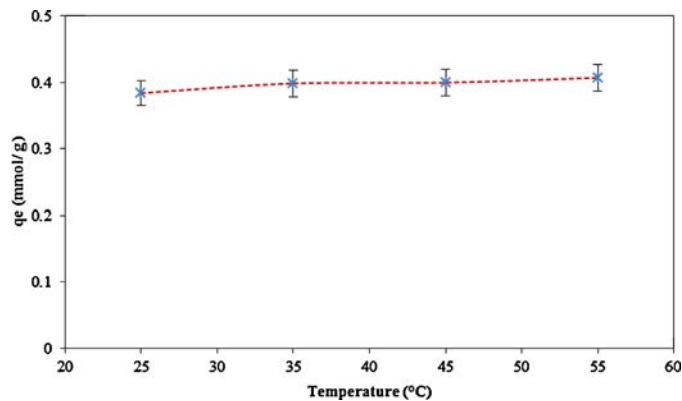


Fig. 11. Effect of temperature, equilibrium time = 60 min, pH = 8, agitation speed = 200 rpm, adsorbent dosage = 0.005 g.

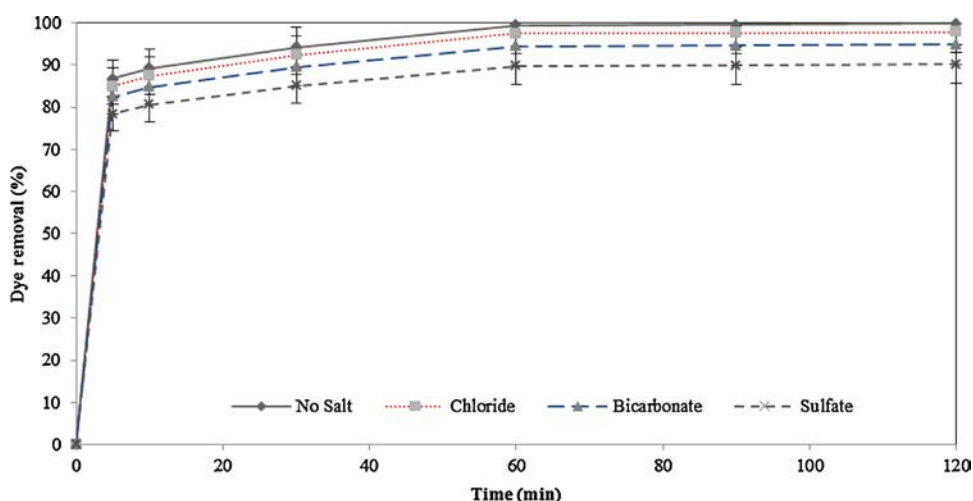


Fig. 12. Effect of salt, equilibrium time = 60 min, pH = 8, agitation speed = 200 rpm, adsorbent dosage = 0.005 g.

3.8. Adsorption isotherms

The distribution of dye between the adsorbent and the dye solution at equilibrium is important in establishing the capacity of the adsorbent for dye removal from aqueous systems. The adsorption isotherms of BR46 on both raw and modified diatomite are shown in Fig. 13. It is clearly seen from Fig. 13 that the amount of adsorbed BR46 on raw diatomite was much lower than that of NONMD.

The experimental data were evaluated by various isotherm models incorporating Langmuir, Freundlich [8–24] and Brunauer–Emmett–Teller (BET)[16–46] isotherms.

Langmuir isotherm is applicable for monolayer adsorption on a surface containing a finite number of identical adsorption sites [24]. A linear expression for the Langmuir isotherm is as follows:

$$1/q_e = \left(\frac{1}{K_L Q_0} \right) (1/C_e) + 1/Q_0 \quad (3)$$

where C_e is the concentration of dye under equilibrium condition (mg/L), q_e denotes the amount of dye adsorbed at equilibrium (mg/g), Q_0 indicates the maximum adsorption capacity and K_L is the Langmuir isotherm constant (l/mg). The values of K_L and Q_0 were calculated from the slope and intercept of the linear plot of $1/q_e$ versus $1/C_e$.

Freundlich equation was also applied for the adsorption of BR46 on diatomite as given below:

$$q_e = K_F C_e^{1/n} \quad (4)$$

where C_e is the equilibrium dye concentration in aqueous system (mg/L), q_e is the amount of dye adsorbed per weight of the adsorbent (mg/g), K_F and n are Freundlich isotherm constants

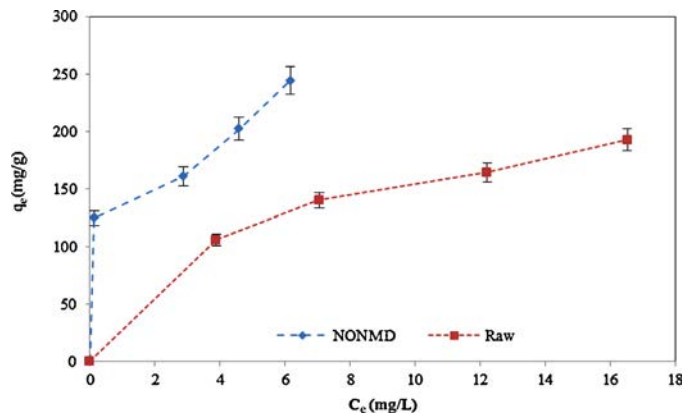


Fig. 13. Adsorption isotherms of BR46 dye onto raw and modified diatomite.

Table 2

Parameters of various isotherms for adsorption of BR46 dye onto raw diatomite and NONMD.

	Langmuir				Freundlich				BET			
	Q_0	K_L	r_1^2	RMSE	K_F	$1/n$	r_2^2	RMSE	K_b	q_m	r_3^2	RMSE
Raw	83.67	0.013	0.9980	0.23	2.76	0.83	0.9891	0.44	-1.94	1.43	0.8991	0.55
NONMD	98.16	0.942	0.9804	0.54	22.58	0.64	0.9837	0.43	17.63	0.0132	0.9998	0.21

Table 3

Kinetics constants for BR46 dye adsorption by raw diatomite and NONMD.

	Pseudo-first-order				Pseudo-second-order			
	q_e (mg/g)	$K_{1,ad}$ (1/min)	R^2	RMSE	q_e (mg/g)	$K_{2,ad}$ (g/mg min)	R^2	RMSE
Raw	123.249	0.835	0.9881	0.123	172.192	0.0143	0.9987	0.115
NONMD	29.52	0.419	0.9901	0.119	115.16	0.046	0.9998	0.112

incorporating all factors affecting the adsorption process. Taking \log_{10} from both sides of the Eq. (4) yields the following equation:

$$\log_{10}q_e = \log_{10}K_F + \frac{1}{n}\log_{10}C_e \quad (5)$$

Linear plot of $\log_{10}q_e$ versus $\log_{10}C_e$ gives the values of K_F and n .

Brunauer–Emmett–Teller (BET) model was also used to fit the adsorption data according to the linear form of its rearranged adsorption isotherm model, which may be expressed as:

$$\frac{C_e}{(C_s - C_e)q_e} = \frac{1}{K_b q_m} + \left(\frac{K_b - 1}{K_b q_m}\right)\left(\frac{C_e}{C_s}\right) \quad (6)$$

where C_e is the concentration of dye in solution (mg/L), C_s denotes the saturation concentration of dye (mg/L), q_e is the amount of dye adsorbed per weight of the diatomite used (mg/g), q_m is the amount of dye adsorbed in forming a complete monolayer (mg/g), and K_b indicates a constant explaining the energy of interaction with the surface. The values of K_b and q_m were calculated from the slope and intercept of the linear plot of $\left(\frac{C_e}{C_s - C_e}\right)\frac{1}{q_e}$ versus $\frac{C_e}{C_s}$.

The Q_0 , K_L , r_1^2 (correlation coefficient for Langmuir isotherm), K_F , $1/n$, r_2^2 (correlation coefficient for Freundlich isotherm), K_b , q_m and r_3^2 (correlation coefficient for BET isotherm) are given in Table 2. The negative values of K_b related to the BET isotherm model describe that the adsorption process for raw diatomite did not follow the BET isotherm, since this constant is indicative of the surface binding energy. It is evident from Table 2 that the isotherm data for the adsorption of BR46 by raw diatomite were best-fitted using Langmuir model with a correlation coefficient of 0.9980. Furthermore, the BET model is most appropriate for the adsorption of BR46 on NONMD with a correlation coefficient of 0.9998. In addition, standard statistics of root mean squared error (RMSE) was carried out to support the best fit adsorption model. RMSE can be expressed as:

$$RMSE = \left[\frac{1}{n} \sum (q_p - q_o)^2\right]^{\frac{1}{2}} \quad (7)$$

where q_p is the predicted sorption capacity (mg/g), q_o is the observed sorption capacity (mg/g) and n is the number of samples. Thus, based on the high R^2 and low RMSE values, the results present that the adsorption of BR 46 on the raw diatomite and the NONMD follow the Langmuir model and the BET model, respectively [49]. It is clear from Table 2 that the adsorption capacity of NONMD is more than raw diatomite. The Langmuir isotherm constants, K_L and the maximum adsorption capacity (Q_0) for NONMD are 72.46 and 1.17 times more than raw one, respectively.

3.9. Adsorption kinetics

The prediction of the adsorption kinetics of dye from aqueous system is important in order to design a suitable treatment system. The kinetics of adsorption of BR46 on diatomite may be described by the pseudo-first-order Lagergren rate equation [16,19,24] and the pseudo-second-order rate expression developed by Ho and McKay [57]. The Lagergren equation is:

$$\log(q_e - q_t) = \log q_e - \frac{K_{1,ad}}{2.303} t \quad (8)$$

where q_e and q_t are the amounts of dye (mg/g) adsorbed at equilibrium and at time t (min) and $K_{1,ad}$ is the pseudo-first-order rate constant (1/min).

The Ho and McKay equation is given below:

$$\frac{t}{q_t} = \frac{1}{K_{2,ad}q_e^2} + \frac{t}{q_e} \quad (9)$$

$K_{2,ad}$ is the rate constant of the pseudo-second-order model (g/mg min). Linear plot of $\log_{10}(q_e - q_t)$ against t gives the rate constant of $K_{1,ad}$. Moreover, the value of $K_{2,ad}$ is obtained from the intercept of the linear plot of t/q_t versus t . Adsorption kinetics constants of the pseudo-first-order and pseudo-second-order models at pH 8, temperature 25 ± 1 °C, agitation speed of 200 rpm, initial concentration of 25 mg/L and for a time period of 60 min are given in Table 3. Table 3 shows that the pseudo-second-order is the predominant kinetic model for both raw and modified diatomite due to high R^2 and low RMSE values [49].

4. Conclusions

In the present investigation, diatomite has been studied for the removal of BR46 from aqueous solution. Modification treatment of the adsorbent was useful which lead to increase its adsorption capacity. The adsorption process was also influenced by solution pH. The maximum sorption capacity occurred at pH 8. The rise in temperature caused a negligible increase in the adsorption efficiency of the NONMD. It was found that under optimum conditions, a maximum removal percentage of 84.49 and 99.48% obtained in the case of BR46 dye removal from aqueous solution in raw and modified diatomite respectively. The capacity of dye removal by NONMD is decreased in the presence of salts in order to compete the small salt molecules with dyes in adsorption onto NONMD. BR 46 adsorption on the raw diatomite and the NONMD follow the Langmuir model and the BET model, respectively. Besides, the pseudo-second-order is the predominant kinetic model for both adsorbents. The results presented here can help to

design an appropriate remediation plan to minimise the unfavourable impacts caused by industrial effluents containing BR46 dye.

Acknowledgments

The authors are thankful to Petroleum University of Technology for providing the financial help and to Institute for Colorants, Paints and Coatings (ICPC), for supporting this research.

References

- [1] Couto SR. Dye removal by immobilised fungi. *Biotechnol Adv* 2009;27:227–35.
- [2] Fu Y, Viraraghavan T. Fungal decolorization of dye wastewaters, a review. *Bioresour Technol* 2001;79:251–62.
- [3] Toh YC, Yen JIL, Jeffrey PO, Ting YP. Decolorisation of azo dyes by whiterot fungus (WRF) isolated in Singapore. *Enzyme Microb Technol* 2003;35:569–75.
- [4] Sivaraj R, Namasivayam C, Kadirvelu K. Orange peel as an adsorbent in the removal of acid violet 17 (acid dye) from aqueous solutions. *Waste Manage* 2001;21:105–10.
- [5] Nacera Y, Aicha B. Equilibrium and kinetic modelling of methylene blue sorption by pretreated dead streptomyces rimosus effect of temperature. *Chem Eng J* 2006;119:121–5.
- [6] Wong Y, Yu J. Laccase catalysed decolorisation of synthetic dyes. *Water Res* 1999;33:3512–20.
- [7] Banat IM, Nigam P, Singh D, Marchant R. Microbial decolorization of textile dye-containing effluents: a review. *Bioresour Technol* 1996;58:217–27.
- [8] Khraisheh MAM, Al-Ghouti MA, Allen SJ, Ahmad MN. Effect of OH and Silanol groups in the removal of dyes from aqueous solution using diatomite. *Water Res* 2005;39:922–32.
- [9] Venkata Mohan S, Sailaja P, Srimurali M, Karthikeyan J. Color removal of monoazoacid dye from aqueous solution by adsorption and chemical coagulation. *Environ Eng Pol* 1999;1:149–54.
- [10] Khalighi Sheshdeh R, Khosravi Nikou MR, Badii Kh, Mohammadzadeh SAT. Evaluation of adsorption kinetics and equilibrium for the removal of benzene by modified diatomite. *Chem Eng Technol* 2013;36:1713–20.
- [11] Chun H, Yizhong W. Decolorization and biodegradability of photocatalytic treated azo dyes and wool textile wastewater. *Chemosphere* 1999;39:2107–15.
- [12] Hachem C, Bocquillon F, Zahraa O, Bouchy M. Decolorization of textile industry wastewater by the photocatalytic degradation process. *Dyes Pigments* 2001;49:117–25.
- [13] Mahmoodi NM, Arami M, Yousefi Limaee N, Salman Tabrizi N. Decolorization and aromatic ring degradation kinetics of Direct Red 80 by UV oxidation in the presence of hydrogen peroxide utilizing TiO₂ as a photocatalyst. *Chem Eng J* 2005;112:191–6.
- [14] Wu J, Eiteman MA, Law SE. Evaluation of membrane filtration and ozonation processes for the treatment of reactive dye wastewater. *J Environ Eng* 1998;124:272–7.
- [15] Pearce CL, Lloyd JR, Guthrie JT. The removal of colour from textile wastewater using whole bacterial cells: a review. *Dyes Pigments* 2003;58:179–96.
- [16] Vlyssides AG, Loizidou M, Karlis PK, Zorpas AA, Papaioannou D. Electrochemical oxidation of a textile dye wastewater using a Pt/Ti electrode. *J Hazard Mater* 1999;70:41–52.
- [17] Khattri SD, Singh MK. Colour removal from synthetic dye wastewater using a bioadsorbent. *Water Air Soil Pollut* 2000;120:283–94.
- [18] Benkli YE, Can MF, Turan M, Çelik MS. Modification of organo-zeolite surface for the removal of reactive azo dyes in fixed-bed reactors. *Water Res* 2005;39:487–93.
- [19] Shawabkeh RA, Tutunji MF. Experimental study and modeling of basic dye sorption by diatomaceous clay. *Appl Clay Sci* 2003;24:111–20.
- [20] Gong R, Ding Y, Li M, Yang C, Liu H, Sun Y. Utilization of powdered peanut hull as biosorbent for removal of anionic dyes from aqueous solution. *Dyes Pigments* 2005;64:187–92.
- [21] Fu Y, Viraraghavan T. Removal of Congo Red from an aqueous solution by fungus *Aspergillus niger*. *Adv Environ Res* 2002;7:239–47.
- [22] Gucek A, Sener S, Bilgen S, Mazmanci ML. Adsorption and kinetic studies of cationic and anionic dyes on pyrophyllite from aqueous solutions. *J Colloid Interf Sci* 2005;286:53–60.
- [23] Wang S, Boyjoo Y, Choueib A, Zhu ZH. Removal of dyes from aqueous solution using fly ash and red mud. *Water Res* 2005;39:129–38.
- [24] Netpradit S, Thiravetyan P, Towprayoon S. Adsorption of three azo reactive dyes by metal hydroxide sludge: effect of temperature, pH, and electrolytes. *J Colloid Interf Sci* 2004;270:255–61.
- [25] Namasivayam C, Arasi DJSE. Recycling of industrial solid waste for the removal of mercury (II) by adsorption process. *Chemosphere* 1997;34:357–75.
- [26] Pala A, Tokat E. Color removal from cotton textile industry wastewater in an activated sludge system with various additives. *Water Res* 2002;36:2920–5.
- [27] Aksu Z. Application of biosorption for the removal of organic pollutants: a review. *Process Biochem* 2005;40:997–1026.
- [28] Shawabkeh R, Al-Harabsheh A, Al-Otoom A. Copper and zinc sorption by treated oil shale ash. *Sep Purif Technol* 2004;40:251–7.
- [29] Lin YH, Leu JY. Kinetics of reactive azo-dye decolorization by *Pseudomonas luteola* in a biological activated carbon process. *Biochem Eng J* 2008;39:457–67.
- [30] Annadurai G, Juang RS, Lee DJ. Factorial design analysis for adsorption of dye on activated carbon beads incorporated with calcium alginate. *Adv Environ Res* 2002;6:191–8.
- [31] Chakraborty S, De S, Das Gupta S, Basu JK. Adsorption study for the removal of a basic dye: experimental and modelling. *Chemosphere* 2005;58:1079–86.
- [32] Khraisheh MAM, Al-degs YS, Mcminn WAM. A remediation of wastewater containing heavy metals using raw and modified diatomite. *Chem Eng J* 2004;99:177–84.
- [33] El-Geundi MS. Colour removal from textile effluents by adsorption techniques. *Water Res* 1991;25:271–3.
- [34] Namasivayam C, Kanchana N. Waste banana pith as adsorbent for colour removal from wastewater. *Chemosphere* 1992;25:1691–705.
- [35] Allen SJ, Gan Q, Matthews R, Johnson PA. Comparison of optimised isotherm models for basic dye adsorption by kuzdu. *Bioresour Technol* 2003;88:143–52.
- [36] Morais LC, Freitas OM, Goncalves EP, Vasconcelos LT, Gonzalez-Beca CG. Reactive dyes removal from wastewaters by adsorption on eucalyptus bark: variables that define the process. *Water Res* 1999;33:979–88.
- [37] Bhattacharyya KG, Sarma A. Adsorption characteristics of the dye, Brilliant green, on Neem leaf powder. *Dyes Pigments* 2003;57:211–22.
- [38] Demir H, Top A, Balkose D, Ulku S. Dye adsorption behaviour of Luffa cylindrical fibers. *J Hazard Mater* 2008;153:389–94.
- [39] Hameed BH. Equilibrium and kinetic studies of methyl violet sorption by agricultural waste. *J Hazard Mater* 2008;154:204–12.
- [40] Arami M, Limaee NY, Mahmoodi NM, Tabrizi NS. Equilibrium and kinetics studies for the adsorption of direct and acid dyes from aqueous solution by soy meal hull. *J Hazard Mater* 2006;B135:171–9.
- [41] Ferrero F. Dye removal by low cost adsorbents: hazelnut shells in comparison with wood sawdust. *J Hazard Mater* 2007;142:144–52.
- [42] Ho YS, McKay G. Sorption of dye from aqueous solution by peat. *Chem Eng J* 1998;70:115–24.
- [43] Khalighi Sheshdeh R, Khosravi Nikou MR, Badii Kh, Yousefi Limaee N. Adsorption of basic organic colorants from an aqua binary mixture by diatomite. *Prog Color Colorants Coat* 2012;5:101–16.
- [44] Angela Y, Danil de Namor F, El Gamouz A, Frangie S, Martinez V, Valiente L, Oliver A. Turning the volume down on heavy metals using tuned diatomite. A review of diatomite and modified diatomite for the extraction of heavy metals from water. *J Hazard Mater* 2012;241:14–31.
- [45] Al-Ghouti M, Khraisheh MAM, Ahmad MNM, Allen S. Thermodynamic behaviour and the effect of temperature on the removal of dyes from aqueous solution using modified diatomite. A kinetic study. *J Colloid Interf Sci* 2005;287:6–13.
- [46] Colgecen G, Erdem E, Donatt R. The removal of textile dyes by diatomite earth. *J Colloid and Int Sci* 2005;282:314–9.
- [47] Hayat K, Gondal MA, Khaled MM. Effect of operational key parameters on photocatalytic degradation of phenol using nano nickel oxide synthesized by sol gel method. *J Mol Catal* 2011;A336:64–71.
- [48] Deniz F, Karaman S. Removal of Basic Red 46 dye from aqueous solution by pine tree leaves. *Chem Eng J* 2011;170:67–74.
- [49] Deniz F, Saygideger SD. Removal of a hazardous azo dye (Basic Red 46) from aqueous solution by princess tree leaf. *Desalin* 2011;268:6–11.
- [50] Bannani Karim A, Mounir B, Hachkar M, Bakasse M, Yaacoubi A. Removal of Basic Red 46 dye from aqueous solution by adsorption onto Moroccan clay. *J Hazard Mater* 2009;168:304–9.
- [51] Olgun A, Atar N. Equilibrium kinetic adsorption study of Basic Yellow 28 and Basic Red 46 by a boron industry waste. *J Hazard Mater* 2009;161:148–56.
- [52] Deniz F, Saygideger SD. Investigation of adsorption characteristics of Basic Red 46 onto gypsum: Equilibrium, kinetic and thermodynamic studies. *Desalin* 2010;262:161–5.
- [53] Gabrovska M, Krstić J, Edreva-Kardjieva R, Stanković M, Jovanović D. The influence of the support on the properties of nickel catalysts for edible oil hydrogenation. *Appl Catal A: Gen* 2006;299:73–83.
- [54] Ozer A, Dursun G. Removal of methylene blue from aqueous solution by dehydrated wheat bran carbon. *J Hazard Mater* 2007;146:262–9.
- [55] Senturk HB, Ozdes D, Duran C. Biosorption of Rhodamine 6G from aqueous solutions onto almond shell (*Prunus dulcis*) as a low cost biosorbent. *Desalin* 2010;252:81–7.
- [56] Senthil Kumar P, Ramalingam S, Senthamarai C, Niranjana M, Vijayalakshmi P, Sivanesan S. Adsorption of dye from aqueous solution by cashew nut shell: studies on equilibrium isotherm kinetics and thermodynamics of interactions. *Desalin* 2010;261:52–60.
- [57] Badii Kh, Doulati Ardejani F, Saberi MA, Yousefi Limaee N, Shafaei SZAT. Adsorption of Acid blue 25 dye on diatomite in aqueous solutions. *Indian J Chem Technol* 2010;17:1–7.
- [58] Mahmoodi NM. Photocatalytic ozonation of dyes using copper ferrite nano-particle prepared by co-precipitation method. *Desalin* 2011;279:332–7.